

# Impact of the snow surface on the ice crystal concentration measurements at mountain-top stations

Alexander Beck<sup>1</sup>, Jan Henneberger<sup>1</sup>, and Ulrike Lohmann<sup>1</sup>

<sup>1</sup>Institute for Atmospheric and Climate Sciences, ETH Zurich, Zurich, Switzerland

## Key Points:

- In-situ measurements of microphysical cloud properties with a holographic Imager
- Influence of in-situ cloud observations at mountain top stations by ground based ice enhancement processes
- •

10 **Abstract**

11 In-situ cloud observations at mountain-top research station regularly measure ice crystal  
 12 number concentrations (ICNCs) orders of magnitudes higher than expected from measure-  
 13 ments of ice nuclei particle concentrations. Several studies suggest that mountain-top in-  
 14 situ measurements are influenced by surface-based ice-enhancement process, e.g. blowing  
 15 snow, hoar frost or riming on snow covered trees, rocks and the remaining snow surface.  
 16 A strong influence of in-situ observations on mountain-top stations by surface-based ice-  
 17 enhancement processes may limit the relevance of such measurements and could have an  
 18 impact on orographic clouds.

19 This study assesses the influence of surface-based ice-enhancement processes on  
 20 in-situ cloud observations at the Sonnblick Observatory in the Hohen Tauern Region,  
 21 Austria. Vertical profiles of ICNCc above a snow covered surface were observed up to  
 22 a height of 10 m. A decrease of the ICNC by at least a factor of two is observed, if the  
 23 maximum ICNC is larger than  $1001^{-1}$ . This decrease can be up to one order of magnitude  
 24 during in cloud conditions and reached its maximum of more than two orders of magni-  
 25 tudes when the station was not in cloud. On one day a similar decrease of regular and  
 26 irregular ice crystals was observed with height, which cannot be explained by surface-  
 27 based ice-crystal enhancement processes. A mechanism is proposed that possibly enhances  
 28 the ICNC close to the surface when cloud particles sediment and are captured in a turbu-  
 29 lent layer above the surface. These observations strongly suggest that mountain-top in-situ  
 30 measurements poorly represent the true properties of the cloud in contact with the surface.  
 31 They are influenced not only by surface-based ice-enhancement processes, but possibly  
 32 also by ICNC enhancement due to turbulent layers above the surface.

33 **1 Introduction**

34 The microphysical properties (e.g. phase composition, cloud particle number con-  
 35 centrations) and cloud processes are key parameters for the clouds lifetime, the cloud ex-  
 36 tent, as well as the intensity of precipitation they produce [Rotunno and Houze, 2007]. For  
 37 example, the phase composition influences the radiative properties of mid-level clouds in  
 38 the temperature range between 0 to -35 °C. Globally, only pure liquid clouds in this tem-  
 39 perature regime reflect  $17 \text{ W m}^{-2}$  more radiation back to space than only ice clouds clouds  
 40 [Lohmann, 2002]. A good representation of orographic mixed-phase clouds is therefore  
 41 crucial for accurate weather predictions in alpine terrain and improved climate models.

42 In-situ measurements are important to further improve our understanding of micro-  
 43 physical properties and fundamental processes of orographic mixed-phase clouds [Baum-  
 44 gardner et al., 2011] and are frequently conducted at mountain-top research stations. De-  
 45 spite an improved understanding on the origin of ice crystals from nucleation [DeMott  
 46 et al., 2015; Boose et al., 2016] as well as from secondary ice-multiplication processes  
 47 [Field et al., 2017], the source of most of the ice crystals observed at mountain-top sta-  
 48 tions and their impact on the development of the cloud remains an enigma [Lohmann  
 49 et al., 2016].

50 In-situ observations with aircraft usually observe ICNC on the order of  $1-101^{-1}$   
 51 [Gultepe et al., 2001], whereas at mountain-top research stations (e.g. Elk Mountain, USA  
 52 or Jungfraujoch, Switzerland) or near the snow surface in the Arctic ICNCs of several  
 53 hundreds to thousands per liter are frequently reported [Rogers and Vali, 1987; Lachlan-  
 54 Cope et al., 2001; Lloyd et al., 2015]. Secondary ice multiplication processes like frag-  
 55 mentation [Rangno and Hobbs, 2001] or the Hallett-Mossop process [Hallet and Mossop,  
 56 1974] are usually ruled out as the source for the observed ice crystals due to the lack of  
 57 large ice crystals, respectively large cloud droplets or the wrong temperature range. In-  
 58 stead surface-based ice-enhancement processes are proposed to produce such enormous  
 59 ICNCs. Rogers and Vali [1987] suggested two possible processes as a source for the ob-  
 60 served ICNC: riming on trees, rocks and the snow surface or the lifting of snow particles

from the surface, i.e. blowing snow. In addition, *Lloyd et al.* [2015] suggested hoar frost as a wind independent, surface-based ice-enhancement process to cause ICNCs larger than  $100\text{I}^{-1}$  for which they did not observe a wind speed dependency as expected for blowing snow. Although different studies are strife about the mechanisms to explain the measured high ICNCs, they agree on a strong influence by surface-based processes.

While the influence of mountain-top measurements by surface-based processes nowadays is accepted, the impact of re-suspended ice crystals on the development of super-cooled orographic clouds, e.g. a more rapid glaciation and enhanced precipitation, has not been studied extensively [*Geerts et al.*, 2015]. If the proposed surface-based ice-enhancement processes have the potential to impact the development of a cloud depends primarily on the penetration depth of the reseuspended particle into a cloud, i.e. the maximum height above the surface to which the particles get lifted.

The height dependency of blowing snow has been studied in the context of snow redistribution ("snow drift") and reduced visibility due to the re-suspended ice crystals by observing ice crystals up to several meters above the snow surface [*Schmidt*, 1982; *Nishimura and Nemoto*, 2005]. It has been reported that blowing snow occurs above a wind speed threshold that varies between  $4\text{ m s}^{-1}$  and  $13\text{ m s}^{-1}$  [*Bromwich*, 1988; *Li and Pomeroy*, 1997; *Mahesh et al.*, 2003; *Déry and Yau*, 1999]. Besides the wind speed, the concentration of blowing snow depends on the snowpack properties (e.g. snow type, time since last snow fall,...) and on the atmospheric conditions (e.g. current temperature, humidity,...) [*Vionnet et al.*, 2013]. *Nishimura and Nemoto* [2005] observed resuspended ice crystals from the surface up to a height of 9.6 m and found that the ICNCs usually decrease to as low as 1-10 particles per liter. During a precipitation event, the relative importance of the small ice crystals below  $< 100\text{ }\mu\text{m}$  decreases from nearly 100 % at 1.1 m to below 20 % at 9.6 m. The rapid decrease of ICNCs with height observed in these studies may limit the impact of blowing snow on orographic clouds. However, most of these studies were conducted in dry air conditions where ice crystals undergo rapid sublimation [*Yang and Yau*, 2008], which may restrict the applicability of these results.

*Lloyd et al.* [2015] suggested that vapor grown ice crystals on the crystalline surface of the snow cover, i.e. hoar frost, may be detached by mechanical fracturing due to turbulence independent of wind speed. To our knowledge only one modelling study exists, which assesses the impact of hoar frost on the development of a cloud. *Farrington et al.* [2015] implemented a flux of surface hoar crystals in the WRF (Weather Research and Forecasting) model based on a frost flower aerosol flux to simulate ICNCs measured at the Jungfraujoch by *Lloyd et al.* [2015]. They concluded that the surface-based ice crystals have a limiting impact on orographic clouds because the ice crystals are not advected high into the atmosphere. However, more measurements of ice crystal fluxes from the snow covered surface are necessary to simulate the impact of surface-based ice crystal enhancement processes on the development of orographic clouds [*Farrington et al.*, 2015].

In contrast to these findings, several remote sensing (i.e. satellite, lidar and radar) studies measured ice crystals advected as high as 1 km above the surface, which suggests an impact of surface-originated ice crystals on clouds. Satellite observations of blowing snow from MODIS and CALIOP over Antarctica [*Palm et al.*, 2011] observed layer thickness up to 1 km with an average thickness of 120 m for all observed blowing snow events. Similar observations from lidar measurements exist from the South Pole with observed layer thicknesses of ice crystals of usually less than 400 m, with some rare cases when a subvisual layer exceeded a height of 1 km [*Mahesh et al.*, 2003]. However, a possible suspension of clear-sky precipitation could not be ruled out as a source of the observed ice crystal layers. Observations of layers of ice crystals from radar measurements on an aircraft in the vicinity of the Medicine Bow Mountains [*Vali et al.*, 2012] observed ground-layer snow clouds which where most of the time not visually detectable but produced a radar signal. Resuspended ice crystals from the surface or riming of cloud droplets at the surface can be the origin of the ice crystals in such ground-layer snow clouds. *Geerts*

114 *et al.* [2015] presented evidence for ice crystals becoming lofted up to 250 m in the atmo-  
 115 sphere by boundary layer separation behind terrain crests and by hydraulic jumps. Also  
 116 evidence that ice crystals from the surface may lead to the glaciation of supercooled orographic  
 117 clouds and enhanced precipitation was found. However, *Geerts et al.* [2015] also  
 118 mentioned the limitation of radar and lidar measurements to separate the small ice crystals  
 119 produced by surface processes from the larger falling snow particles and more abundant  
 120 cloud droplets. They even concluded, that "to explore BIP (blowing snow ice particle)  
 121 lofting into orographic clouds, ice particle imaging devices need to be installed on a tall  
 122 tower, or on a very steep mountain like the Jungfraujoch".

123 In this study we assess the influence of surface-based ice-enhancement processes on  
 124 in-situ cloud observations at mountain-top stations and the potential impact on orographic  
 125 mixed-phase clouds. Vertical profiles of the ICNC up to a height of 10 m above the sur-  
 126 face were observed for the first time on a high-altitude mountain station with the holo-  
 127 graphic imager HOLIMO [*Beck et al.*, 2017]. HOLIMO is capable of imaging ice crystals  
 128 larger than 25  $\mu\text{m}$  and the shape of these ice crystals can be analyzed.

## 129 2 Field Measurements at the Sonnblick Observatory

### 130 2.1 Site description

131 This field campaign was conducted at the Sonnblick Observatory (SBO) situated at  
 132 the summit of Mt. Sonnblick at 3106 masl (12°57'E, 47°3'N) in the Hohen Tauern Na-  
 133 tional Park in the Austrian Alps. The SBO is a meteorological observatory operated all  
 134 year by the ZAMG (Central Institute for Meteorology and Geodynamics). On the east and  
 135 south the SBO is surrounded by large glacier fields with a moderate slope, whereas on the  
 136 northeast a steep wall of approximately 800 m descends to the valley (Fig. 1, right). Part  
 137 of the SBO is a 15 m high tower used for meteorological measurements by the ZAMG.  
 138 The data presented in this paper was collected during a field campaign in February 2017.

### 139 2.2 Instrumentation

140 The properties of hydrometeors were observed with the holographic imager HOLIMO,  
 141 which is part of the HoloGondel platform [*Beck et al.*, 2017]. The holographic imager was  
 142 mounted on an elevator that was attached to the meteorological tower of the SBO (Fig. 2)  
 143 to obtain vertical profiles of the hydrometeor properties up to a height of 10 m above the  
 144 surface where the platform was repeatedly positioned at five different heights as indicated  
 145 in Figure 2. The holographic imager HOLIMO had a distance of approximately 1.5 m  
 146 from the tower on the east-northeast side of the tower (Fig. 1, right).

147 The holographic imager HOLIMO yields single particle informations, e.g. size, and  
 148 shadowgraphs from all cloud particles in a three-dimensional volume on a single image,  
 149 a so-called hologram. Per hologram, a sample volume of 16  $\text{cm}^3$  with a length of 6 cm  
 150 along the optical axis is examined. Concentrations and particle size distributions are cal-  
 151 culated over 50 holograms corresponding to a volume of 800  $\text{cm}^3$ . The open source soft-  
 152 ware HoloSuite [*Fugal*, 2017] is used to reconstruct the in-focus images of the particles.  
 153 Particles smaller than 25  $\mu\text{m}$  are classified as liquid droplets, whereas particles larger than  
 154 25  $\mu\text{m}$  are separated in liquid droplets and ice crystals based on the shape of their 2D im-  
 155 age. Similar to a study by *Schlenzeck and Fugal* [2017] the ice crystals were further vi-  
 156 sually classified into three different groups: regular, irregular and aggregates. Because  
 157 the visual classification of several thousands of ice crystals is time consuming this sub-  
 158 classification of ice crystals was done only for the profiles on February 17th.

159 A single vertical profile was observed within a time interval of 10-12 min. By posi-  
 160 tioning the holographic imager HOLIMO was positioned at an individual height for 2 min  
 161 and recording holograms at 4 fps. This results in 81 of sampled air.

162 Meteorological data are available from the measurements by the ZAMG. The ZAMG  
 163 measures one minute averages of temperature, relative humidity and horizontal wind speed  
 164 and direction at the top of the meteorological tower. Snow cover depth is daily manually  
 165 observed by the operators of the SBO. Based on these measurements the change of the  
 166 snow cover is calculated. However, this calculation includes all the changes in the snow  
 167 cover depth, e.g. snow drift, sublimation, melting and fresh snow. Daily measurements of  
 168 the total precipitation are available on the north and south side of the SBO. A ceilometer  
 169 located in the valley north of the SBO measured the cloud base and cloud depth.

170 In addition, a 3D sonic anemometer was mounted at the top of the meteorological  
 171 tower. However, data is only available occasionally, because most of the time the heating  
 172 of the anemometer was not sufficient to prevent the build up of rime on the measurement  
 173 arms.

### 174 3 Results

175 The data presented were observed on 4 February and 17 February, 2017. Figure 3  
 176 and 4 show an overview on the meteorological conditions on both days. The main differ-  
 177 ence is the wind direction, which was south-west on 4 February and north on 17 February.

#### 178 3.1 Case study on 4 February, 2017

179 On 4 February a low pressure system moved eastwards from the Atlantic Ocean  
 180 over northern France to western Germany, where it slowly dissipated. Influenced by this  
 181 low pressure system the wind at the SBO predominantly came from west-southwest and  
 182 wind speeds were between 10 and 25 m s<sup>-1</sup> (Fig. 3). In the late afternoon, around 1900  
 183 UTC, when the low pressure system dissipated over western Germany, the wind direction  
 184 changed to north and wind speeds decreased to a minimum of 5 m s<sup>-1</sup>. After 1900 UTC  
 185 wind speed increased again to up to 15 m s<sup>-1</sup>. Starting from 0800 UTC the SBO was in  
 186 cloud except for a short time interval between 1910 and 2020 UTC. Because no data is  
 187 available from the 3D sonic anemometer, only one minute averages are available from the  
 188 ZAMG measurements.

189 The temperature did not change much during the day and stayed between -10 and  
 190 -9 °C until 1900 UTC when the wind direction changed to north and the temperature de-  
 191 creased to -11 °C at 22 UTC.

192 Between 0830 and 2200 UTC, a total of 24 vertical profiles was obtained, whereas  
 193 the SBO was in cloud except for a short time period between 1910 and 2020 UTC (blue  
 194 shaded in Fig. 3). The ICNC reached a maximum at 2.5 m above the surface (Fig. 5).  
 195 Compared to this maximum, the mean ICNC at a height of 10 m decreases by a factor of  
 196 two and the median ICNC even by a factor of four. This strong decreased of ICNC with  
 197 height suggests that the majority of the ice crystals near the ground originate from the  
 198 snow surface.

199 The whole measurement time period on February 4th was divided in four periods  
 200 representing different conditions (Fig. 6). Between 1910 and 2010 UTC (Fig. 6 third  
 201 row), when the SBO was not in cloud, the ICNC has its maximum at a height of 2.5 m,  
 202 where it reaches up to 600 l<sup>-1</sup>. For three of the profiles, the ICNC decrease by more than  
 203 a factor of 5 from over 100 l<sup>-1</sup> at 2.5 m to less than 20 l<sup>-1</sup> at 10 m. The mean ICNCs de-  
 204 creases from around 100 l<sup>-1</sup> at 2.5 m to 10 l<sup>-1</sup> at 10 m (Fig. 6, right panel in the third  
 205 row). The large extent of the shaded area at 2.5 m represents the high variability of the  
 206 ICNC even when the data is averaged over 800 cm<sup>3</sup>. Because the SBO was not in cloud  
 207 during this time period, these measurements strongly suggest that up to several hundreds  
 208 of ice crystals per liter originated from surface-based processes at a height of 2.5 m and at  
 209 a wind speed of less than 10 m s<sup>-1</sup>.

210 Between 2030 and 2200 UTC (Fig. 6 first row), when the SBO was in cloud again,  
 211 the vertical profiles of the ICNC show a similar tendency as in the cloud free period. The  
 212 maximum of the ICNC was observed at a height of 4.1 m and the ICNC decreased consistently  
 213 for all four profiles with height. The mean of the ICNC decreased by a factor of 9  
 214 from its maximum at 4.1 m to its minimum at 10 m. This decrease is on the same order of  
 215 magnitude as in the cloud free case discussed above. Assuming that the observed ICNC at  
 216 10 m is representative for the cloud without surface influence, the surface-based processes  
 217 contribute with several hundreds of ice crystals per liter to the measurements at 2.5, 4.1  
 218 and 6.0 m. This surface-based contribution is on the same order of magnitude as the total  
 219 measured ICNCs in the cloud free period observed between 1910 and 2020 UTC. In  
 220 contrast to the cloud free period, the surface influence now extends to a height of 6.0 m,  
 221 which can be explained by the increased wind speed of up to  $15 \text{ m s}^{-1}$ .

222 The highest ICNCs were observed in the time period between 1200 and 1500 UTC  
 223 (Fig. 6 second row) when also the wind speed reached its maximum of  $25 \text{ m s}^{-1}$ . The  
 224 boxplot shows a maximum ICNC at 2.5 m in the range of  $500$  to  $900 \text{ l}^{-1}$  and a decrease  
 225 by a factor of 2 within 7.5 m. This decrease is much lower than observed in the previous  
 226 time interval and is most likely due to the high wind speeds. Between different profiles  
 227 the ICNC changed by a factor of ???, however, consistently for all profiles a decreasing  
 228 ICNC was observed with height.

229 In the morning between 0830 and 1100 UTC the observed ICNCs (Fig. 6 first row)  
 230 are much lower than between 1200 and 1500 UTC, although wind speeds were as high as  
 231  $20 \text{ m s}^{-1}$ . A possible reason is that the last snow fall was observed 3 days before the  
 232 measurements. During these time, the loose ice crystals at the surface where blown away and  
 233 the snowpack was solidified by temporal melting and re-freezing of the snowpack. Conse-  
 234 quently, higher wind speeds are necessary to re-suspend ice crystals from the snowpack.

235 The correlation between wind speed and ICNC for 1 min time intervals is shown in  
 236 Figure 7. The maximum wind speeds is used rather the average wind speed, because it  
 237 is expected that the gusts, i.e. the highest wind speed in a time interval are most relevant  
 238 for resuspending ice crystals from the surface. For the time interval between 0830 and  
 239 1500 UTC when the wind direction was west-southwest no correlation is observed with  
 240 wind speeds higher than  $14 \text{ m s}^{-1}$  (Fig 7, top). For the time interval between 1910 and  
 241 2230 UTC, when the wind direction was north, a much more pronounced dependency of  
 242 the ICNC on wind speed is observed for wind speeds lower than  $14 \text{ m s}^{-1}$  (Fig 7, bottom).  
 243 ICNCs reached a saturation for wind speed larger than  $14 \text{ m s}^{-1}$ .

### 244 3.2 17 February 2017

245 On 17 February a cold front over northern Europe was moving southwards causing  
 246 mainly northerly flow across the Alps and at the SBO (Fig. 4). Wind speeds observed at  
 247 the SBO in the time interval between 1800 and 2000 UTC were between  $5$  and  $10 \text{ m s}^{-1}$ .  
 248 In the same time interval temperature decreased by 1 K from  $-12.5$  to  $-13.5^\circ\text{C}$ . The SBO  
 249 was in cloud starting from 1300 UTC with varying visibility between several meters up to  
 250 several hundreds of meters. Some snow fall was observed in the afternoon between 1300  
 251 and 1500 UTC.

252 For this day, wind data of the 3D Sonic Anemometer are available, which allow a  
 253 more detailed analysis of the correlation between the observed ICNC and wind speed. Un-  
 254 fortunately, only four vertical profiles were obtained due to hardware problems with the  
 255 computer. The first profile was measured in the morning at 1200 UTC when the SBO was  
 256 not in cloud and no ice crystals were observed. Three more profiles were observed in the  
 257 late afternoon starting from 1800 UTC. For these profiles the ice crystals have been classi-  
 258 fied by hand and subclassified in the three categories: regular, irregular and aggregates.

The three profiles observed in the late afternoon of 17 February showed ICNCs of several hundreds in the lowest height intervals with a maximum between 4.1 and 6.0 m (Fig. 8). The minimum ICNC was consistently observed for all profiles at 10 m and was always below  $150\text{ l}^{-1}$ . The decrease of the ICNC with height varies between a factor of 2 and 4. In general the observed profiles on this day are similar to the ones observed on 4 February between 2030 and 2200 UTC when similar meteorological conditions were present. Wind direction was mainly north to northeast and wind speed varied between 5 and  $10 \text{ m s}^{-1}$  in both measurement intervals. Only temperature was slightly lower on 17 February.

In contrast to the data of 4 February, no correlation between ICNCs and the horizontal wind speed is observed (Fig. 9). This holds true for the one minute averages and maximum wind speeds observed by the SBO as well as the one second averages observed with the 3D sonic anemometer. However, ICNC increased with the vertical wind speed.

All the ice crystals observed on 17 February were classified by hand into aggregates, irregular and regular ice crystals (Fig. 10). ICNCs are dominantly irregular ice crystals, which is in good agreement with various other observations (citations). However, it is surprising that the fraction of irregular ice crystals stays constant with height or even increases (Fig. 10 right panels). Surface-based ice crystal enhancement processes are expected to produce irregular ice crystals. With increasing height this influence is expected to decrease and regular ice crystals are expected to become more important. However, from this data a proportional decrease of the absolute number of regular and irregular ice crystals is observed and is in contradiction to the expectations from surface-based ice-crystal enhancement processes. A further discussion of there results will follow in section 4.1. The wind speed dependency of irregular and regular ice ICNCs is comparable, and both increase by a factor of 2 when the vertical wind speed increases from  $0\text{--}2 \text{ m s}^{-1}$  to  $4\text{--}6 \text{ m s}^{-1}$  (Fig. 11). Whereas the shape of the size distribution of the irregular ice crystals does not vary much with height, larger regular ice crystals are more strongly reduced with height than smaller regular ice crystals (Fig. 12).

## 4 Discussion

### 4.1 Comparison with the properties of blowing snow observed in the Arctic

To better understand if the observed ice crystals are re-suspended from the surface, the results of 17 February, 2017 are compared to the properties of blowing snow observed in the Arctic ([*Nishimura and Nemoto*, 2005]) and further discussed.

It is expected that the majority of the ice crystals re-suspended from the surface has irregular habits, whereas regular ice crystals originated in cloud. Furthermore, for the re-suspended ice crystals a decrease of ICNC is expected with height, with a stronger decrease of the larger ice crystals. This results in a shift of the size distribution to smaller sizes or a decrease of the mean particle diameter with height, as it was also observed by *Nishimura and Nemoto* [2005]. However, the strongest decrease of the size of the ice crystals was observed below 1 m above the snow surface, whereas the size of the ice crystals stayed fairly constant in the range of  $70\text{--}100 \mu\text{m}$  between 1 and 9.6 m above ground. It is important to notice that *Nishimura and Nemoto* [2005] measured the properties of blowing snow above a flat surface in dry air. Sublimation of ice crystals in such an environment additionally reduces the ice crystal diameter.

For a better comparison a two-parameter gamma probability density function (gamma-pdf) [Budd, 2013; Schmidt, 1982]

$$f(d) = \frac{d^{\alpha-1}}{\beta^\alpha \Gamma(\alpha)} \exp\left(-\frac{\beta}{d}\right) \quad (1)$$

306 with the particle diameter  $d$ , the shape parameter  $\alpha$  and the scale parameter  $\beta$  is  
 307 fitted to the results of 17 February for both regular and irregular ice crystals (Fig. 13).  
 308 The resulting shape parameter  $\alpha$  and the mean diameter, represented by the product of the  
 309 shape and scale parameter of the gamma-pdf, are plotted in Figure 14.

310 The mean diameter for both the irregular and regular ice crystals is in the range of  
 311 the properties of blowing snow, with a decrease from 120 to 70  $\mu\text{m}$  for regular ice crys-  
 312 tals and a rather constant mean diameter of 100  $\mu\text{m}$  for irregular ice crystals (Figure 14  
 313 left). *Nishimura and Nemoto* [2005] observed a strong increase of the shape factor from  
 314 3 to 10 between 1 and 9.6 m. Whereas the shape parameter obtained for the regular ice  
 315 crystals increases with height, it stays constant for the irregular ice crystals. Most impor-  
 316 tant a decrease of the ICNC for both the irregular and regular ice crystals by a factor of  
 317 2 is observed within a height interval of 7.5 m (Fig. 8). All these findings suggest that  
 318 the majority of the irregular as well as the regular ice crystals are re-suspended from the  
 319 snow surface. However, this contradicts our assumptions that the majority of the regular  
 320 ice crystals originate in cloud and only irregular ice crystals are re-suspended from the  
 321 surface, as it is observed between 1910 and 2000 UTC on 4 February. Here an inspection  
 322 of the ice crystal habits by eye showed almost exclusively irregular crystals and therefore  
 323 this is considered a blowing snow event. As a consequence, either our assumptions are  
 324 wrong and also regular ice crystals contribute to the ICNC of re-suspended particles or a  
 325 different mechanism has to be responsible for the enriched ICNC close to the snow sur-  
 326 face (Fig. 10).

327 During the measurements on 17 February the SOB was in cloud. Ice crystals of ir-  
 328 regular and regular habits from the cloud sediment and may be kept floating near the  
 329 surface due to turbulence, which is also responsible for the re-suspension of ice crystals from  
 330 the surface. However, in this case the sedimenting particles may have never reached the  
 331 surface and maintained their habit. Such an effect may also enrich ice crystals observed  
 332 close to the surface, but in this case a snow covered surface is not necessary and the wind  
 333 threshold is much lower than for surface-based ice crystal enhancement processes, because  
 334 ice crystals do not have to be detached from the surface. This can explain the observa-  
 335 tion of high ICNCs on 17 February, where the wind speed was in most cases close to  
 336 the lower threshold wind speed observed for blowing snow, which is  $4 \text{ m s}^{-1}$  [Bromwich,  
 337 1988; Li and Pomeroy, 1997; Mahesh et al., 2003; Déry and Yau, 1999]. The result of such  
 338 a mechanism is a rather constant ICNC above the surface and a similar decrease of the  
 339 ICNC of regular and regular ice crystals with height, as it was observed on 17 February.

340 Although it is proposed that the ICNC is dominated by a mechanism just described,  
 341 blowing snow still contributes to the ICNC at certain time intervals. During one profile  
 342 (Fig. 10, top row) the ICNC decreases for irregular and regular ice crystals with one ex-  
 343 ception for the irregular ice crystals at a height of 6 m. Whereas the vertical wind speed  
 344 during this profile was similar for all heights at  $4 \text{ m s}^{-1}$ , it reached a maximum of  $5.5 \text{ m s}^{-1}$   
 345 when the elevator was positioned at 6 m, corresponding to the increased ICNC of the ir-  
 346 regular ice crystals. The concentration of regular ice crystals was not affected. This sug-  
 347 gests that ice crystals re-suspended from the surface have reached the height of 6 m during  
 348 higher wind speeds and had dominantly irregular habits.

349 The difference in the height dependence of the size distribution of regular and irreg-  
 350 ular ice crystals remains unexplained. Whereas the irregular ice crystals show a constant  
 351 decrease of the ICNC at all sizes, the size distribution for regular ice crystals is shifted to  
 352 smaller sizes with increasing height. A possible reason for the decrease of the mean diam-  
 353 eter of the regular ice crystals is that the particles in the turbulent layer above the surface  
 354 grow due to vapor diffusion before they final fall out. Therefore regular ice crystals closer  
 355 to the surface are larger than the regular ice crystals in cloud. The shift of the size distri-  
 356 bution is then caused by smaller ice crystals that just sediment and have not been captured  
 357 in the turbulent layer. The smaller ice crystals become more important with height and  
 358 start to dominate the size distribution.

359    **4.2 Wind dependence of the observed ICNCs**

360    The observations on 4 February and 17 February show a different correlation of the  
 361    ICNC with wind speed. The ICNCs observed on 4 February show a dependence only for  
 362    horizontal wind speeds below  $14 \text{ m s}^{-1}$  (Fig. 9), whereas for horizontal wind speeds larger  
 363    than  $14 \text{ m s}^{-1}$  this correlation is not observed probably due to a saturation of blowing  
 364    snow. On 17 February a correlation is only observed with vertical wind speed available  
 365    from the 3D sonic anemometer (Fig. 9). Possibly, the vertical wind speed is a better ap-  
 366    proximation for the turbulence responsible for the re-suspension of ice crystals from the  
 367    surface as it was already suggested by Hammer *et al.* [2014]. In addition vertical wind  
 368    speeds play an important role especially at research stations like the SBO and the High  
 369    Altitude Research Station Jungfraujoch, Switzerland, because ice crystals could nucleate  
 370    on suitable INP and/or be transported from below the research station to the measurement  
 371    point. For example [Lloyd *et al.*, 2015] observed a dependence on horizontal wind speeds  
 372    only for ICNCs smaller than  $100 \mu\text{m}$ , whereas larger ICNCs did not show a dependence  
 373    on horizontal wind speed. Blowing snow, respectively hoar frost, was proposed as the un-  
 374    derlying mechanisms for these observations. We suggest that the larger ice crystals ob-  
 375    served by Lloyd *et al.* [2015] have been transported for a longer time and grown to larger  
 376    sizes. In this case the vertical wind speed could be more relevant, because the particles  
 377    may have been transported from below the research station by vertical winds.

378    It has to be mentioned that various difficulties exist when it comes to observing the  
 379    correlation between wind speed and ICNCs. Firstly, ICNCs are usually compared to a  
 380    simultaneously measured wind speed. However, the observed ice crystals have been re-  
 381    suspended some time before the measurement and transported in the air for some time. In  
 382    this case the simultaneously observed wind speed is not necessarily the driving force of  
 383    the process of particle lifting, because ice crystals that were re-suspended from the surface  
 384    by strong turbulence can be transported higher in the atmosphere by much smaller wind  
 385    speeds (blowing snow paper). Secondly, wind and ICNC measurements may be performed  
 386    at two different locations. Especially at mountain-top research station with its many struc-  
 387    tures, local turbulence responsible for the re-suspension of the observed ice crystals may  
 388    be not well represented by such a wind measurement. This is also true for this study,  
 389    where the wind measurement was located on a 15 m high meteorological tower. Thirdly,  
 390    the resuspended ICNC does not only depend on wind speed, but also on age of the snow  
 391    cover and atmospheric conditions and a possible correlation may be suppressed in a data  
 392    set with different snowpack and atmospheric conditions. Between 1900 and 2030 UTC on  
 393    4 February a decrease of the ICNC was observed with time at a height of 2.5 m, possibly  
 394    because the very loose ice crystals on top of the snow cover were blown away.

395    Another crucial point for correlating observed ICNCs to wind speed is the averag-  
 396    ing time of the data. If the averaging time is small, e.g. 1 min it is assumed that the ob-  
 397    served ice crystals were re-suspended close to the measurement point and immediately  
 398    transported. If the averaging time is very large, the effect of blowing snow may be aver-  
 399    aged out. In this study we chose an average time of 10-15 s. This assumes that the par-  
 400    ticles were re-suspended at most 50-100 m upwind from the measurement point and it is  
 401    believed that also peaks of large concentrations are not yet averaged out.

402    **4.3 Influence of ICNC measurements by a snow surface at mountain-top stations  
 403    and its impact on clouds**

404    The results obtained in this study suggest a strong enhancement of the ICNC mea-  
 405    sured close to the snow surface at mountain-top research stations. On 4 February a blow-  
 406    ing snow event was observed when the SBO was not in cloud and the ICNC was en-  
 407    hanced by a factor of 100 at a height of 2.5 m when compared to upper levels of the el-  
 408    evator (Fig. 6, second row). When the SBO was in cloud an enhancement by a factor of  
 409    2-10 was observed in the same height interval. On 17 February a similar decrease of the

410 ICNC was observed for irregular and regular ice crystals. This is in contrast to the ex-  
 411 pectations for blowing snow and a different mechanism is proposed, which enhances the  
 412 ICNC close to the surface when sedimenting ice crystals are captured in turbulence. The  
 413 observed ICNC close to the surface is also at least 2 times larger than at a height of 10 m.  
 414 Therefore, we propose that measurements of the ICNC close to the surface do not repre-  
 415 sent real cloud properties.

416 An estimation of the influence of cloud properties by re-suspended ice crystals is  
 417 difficult, because of the limited vertical extent of the profiles obtained in this study. For  
 418 most of the profiles the ICNC still shows a decreasing tendency at a height of 8-10 m and  
 419 a final statement of the in-cloud ICNC is not possible. Only for the profiles after 1900  
 420 UTC a constant ICNC is observed for the upper levels of the elevator (Fig. 6, two bot-  
 421 tom rows). From the observation between 2030 and 2200 UTC, when the SOB was in  
 422 cloud, the in-cloud ICNC can be estimated, when the observed ICNC during the blowing  
 423 snow event between 1900 and 2000 UTC is subtracted for the upper levels of the eleva-  
 424 tor. This results in a ICNC of several tens per liter. Between 1200 and 1500 UTC (Fig.  
 425 6, second row) the wind speed was much higher and the influence of blowing snow pos-  
 426 sibly extended much higher up in the atmosphere. Because the number of ice nucleating  
 427 particles in clouds is on the order of  $1-101^{-1}$ , already ice crystals of the same concentra-  
 428 tion re-suspended from the surface and lifted high up into the cloud can have a significant  
 429 impact on the clouds properties, e.g. extent and lifetime.

430 To better understand the mechanisms that are responsible for an enhanced ICNC  
 431 close to the surface and to further investigate the mechanisms proposed in this study we  
 432 suggest a more thorough field campaigned with additional 3D sonic anemometers at the  
 433 surface to capture turbulence that may be responsible for the re-suspension of ice crystals,  
 434 a second 3D sonic anemometer on the elevator and a third 3D anemometer on the top of  
 435 the tower. This may help to better understand the wind dependence of the ICNC and to  
 436 find the origin of the observed ice crystals. At best at three cloud imaging probes are part  
 437 of such a campaign and installed parallel to the 3D sonic anemometer. In addition, to get  
 438 a better estimate of the impact of re-suspended particle on cloud porperties, especially for  
 439 high wind speeds, the vertical profiles have to be extended to larger heights above the sur-  
 440 face. Such a field campaign could be conducted using a tethered balloon system equipped  
 441 with cloud imaging probes, which can be lifted several hundreds of meters into the atmo-  
 442 sphere.

## 443 5 Conclusion & Outlook

444 This study assessed the influence of mountain-top in-situ measurements by surface-  
 445 based ice-crystal sources and possible implications on atmospheric relevance of such mea-  
 446 surements. An elevator was attached to the meteorological tower of the SBO, Austria and  
 447 vertical profiles of the ICNC were observed with the holographic imager HOLIMO on two  
 448 days in February 2017. The main findings are:

- 449 • ICNCs decrease with height. ICNCs near the ground are at least a factor of two  
 450 larger than at a height of 10 m (if the ICNC near the ground is larger than  $1001^{-1}$ ).  
 451 The increase in ICNCs near the ground can be up to an order of magnitude during  
 452 cloud events and even two magnitudes during cloud free periods. Therefore, in-situ  
 453 measurements of the ICNC at mountain-top research stations close to the surface  
 454 overestimate the ICNC.
- 455 • On 4 February ICNCs show a dependence on wind speed for wind speeds up to  
 456  $14 \text{ ms}^{-1}$ . For higher wind speeds the ICNCs due to surface-based ice-crystal en-  
 457 hancement processes are possibly saturated.
- 458 • On 17 February a similar decrease of the concentration of irregular and regular ice  
 459 crystals is observed with height, which cannot be explained by surface-based ice  
 460 crystal enhancement processes. Sedimenting ice crystals are possibly captured in a

turbulent layer close to the surface and that enhances ICNCs similarly to blowing snow. However, because the ice crystals actually never had contact with the surface, their habits are preserved.

- The strong influence of surface-based ice-crystals sources on the ICNC measurements on mountain-top stations limits the atmospheric relevance of such measurements. However, the data set obtained is too small to make a clear statement under which conditions in-situ measurements at mountain-top research station may well represent the real properties of a cloud in contact with the surface and when not.
- Further and more extensive field campaigns are necessary to better understand the mechanisms, which are responsible for the enhanced ICNC observed close to the surface at mountain-top research stations and their impact on cloud properties, e.g. extend, lifetime and precipitation initiation.

## 473 Acronyms

- 474 **ICNC** Ice Crystal Number Concentration  
 475 **HOLIMO** HOlographic Imager for Microscopic Objects  
 476 **SBO** Sonnblick Observatory

## 477 Acknowledgments

478 Sonnblick Observatory and team (Elke Ludewig, Hermann Scheer, Norbert Daxbacher,  
 479 Lug Rasser, Hias Daxbacher)  
 480     Thanks to Hannes, Olga, Fabiola, Monika, for their help  
 481     Thanks to Rob for many discussions

## 482 References

- 483 Baumgardner, D., J. Brenguier, A. Bucholtz, H. Coe, P. DeMott, T. Garrett, J. Gayet,  
 484 M. Hermann, A. Heymsfield, A. Korolev, M. KrÃdmer, A. Petzold, W. Strapp,  
 485 P. Pilewskie, J. Taylor, C. Twohy, M. Wendisch, W. Bachalo, and P. Chuang (2011),  
 486 Airborne instruments to measure atmospheric aerosol particles, clouds and radiation:  
 487 A cook's tour of mature and emerging technology, *Atmos. Res.*, 102(1â€¢2), 10 – 29,  
 488 doi:10.1016/j.atmosres.2011.06.021.  
 489 Beck, A., J. Henneberger, S. Schöpfer, J. Fugal, and U. Lohmann (2017), Hologondel, *At-*  
 490 *mos. Meas. Tech.*  
 491 Boose, Y., A. Welti, J. Atkinson, F. Ramelli, A. Danielczok, H. G. Bingemer, M. Plötze,  
 492 B. Sierau, Z. A. Kanji, and U. Lohmann (2016), Heterogeneous ice nucleation on dust  
 493 particles sourced from nine deserts worldwide – part 1: Immersion freezing, *Atmo-*  
 494 *spheric Chemistry and Physics*, 16(23), 15,075–15,095, doi:10.5194/acp-16-15075-2016.  
 495 Bromwich, D. H. (1988), Snowfall in high southern latitudes, *Reviews of Geophysics*,  
 496 26(1), 149–168, doi:10.1029/RG026i001p00149.  
 497 Budd, W. F. (2013), *The Drifting of Nonuniform Snow Particles1*, pp. 59–70, American  
 498 Geophysical Union, doi:10.1029/AR009p0059.  
 499 DeMott, P. J., A. J. Prenni, G. R. McMeeking, R. C. Sullivan, M. D. Petters, Y. Tobe,  
 500 M. Niemand, O. Möhler, J. R. Snider, Z. Wang, and S. M. Kreidenweis (2015), Inte-  
 501 grating laboratory and field data to quantify the immersion freezing ice nucleation ac-  
 502 tivity of mineral dust particles, *Atmospheric Chemistry and Physics*, 15(1), 393–409,  
 503 doi:10.5194/acp-15-393-2015.  
 504 Déry, S. J., and M. K. Yau (1999), A climatology of adverse winter-type weather  
 505 events, *Journal of Geophysical Research: Atmospheres*, 104(D14), 16,657–16,672, doi:  
 506 10.1029/1999JD900158.

- Farrington, R. J., P. J. Connolly, G. Lloyd, K. N. Bower, M. J. Flynn, M. W. Gallagher, P. R. Field, C. Dearden, and T. W. Choularton (2015), Comparing model and measured ice crystal concentrations in orographic clouds during the inupiaq campaign, *Atmos. Chem. and Phys.*, 15(18), 25,647–25,694, doi:10.5194/acpd-15-25647-2015.
- Field, P. R., R. P. Lawson, P. R. A. Brown, G. Lloyd, C. Westbrook, D. Moisseev, A. Miltenberger, A. Nenes, A. Blyth, T. Choularton, P. Connolly, J. Buehl, J. Crosier, Z. Cui, C. Dearden, P. DeMott, A. Flossmann, A. Heymsfield, Y. Huang, H. Kalesse, Z. A. Kanji, A. Korolev, A. Kirchgaessner, S. Lasher-Trapp, T. Leisner, G. McFarquhar, V. Phillips, J. Stith, and S. Sullivan (2017), Secondary ice production: Current state of the science and recommendations for the future, *Meteorological Monographs*, 58, 7.1–7.20, doi:10.1175/AMSMONOGRAPH-D-16-0014.1.
- Fugal, J. P. (2017), Holosuite, in preparation.
- Geerts, B., B. Pokharel, and D. a. R. Kristovich (2015), Blowing Snow as a Natural Glaciogenic Cloud Seeding Mechanism, *Mon. Weather Rev.*, 143(12), 5017–5033, doi:10.1175/MWR-D-15-0241.1.
- Gultepe, I., G. Isaac, and S. Cober (2001), Ice crystal number concentration versus temperature for climate studies, *International Journal of Climatology*, 21(10), 1281–1302, doi:10.1002/joc.642.
- Hallet, J., and S. Mossop (1974), Production of secondary ice particles during the riming process, *Nature*, 249, 26–28, doi:10.1038/249026a0.
- Hammer, E., N. Bukowiecki, M. Gysel, Z. Jurányi, C. R. Hoyle, R. Vogt, U. Baltensperger, and E. Weingartner (2014), Investigation of the effective peak supersaturation for liquid-phase clouds at the high-alpine site jungfraujoch, switzerland (3580 m a.s.l.), *Atmospheric Chemistry and Physics*, 14(2), 1123–1139, doi:10.5194/acp-14-1123-2014.
- Lachlan-Cope, T., R. Ladkin, J. Turner, and P. Davison (2001), Observations of cloud and precipitation particles on the avery plateau, antarctic peninsula, *Antarctic Science*, 13(3), 339–348, doi:10.1017/S0954102001000475.
- Li, L., and J. W. Pomeroy (1997), Estimates of threshold wind speeds for snow transport using meteorological data, *Journal of Applied Meteorology*, 36(3), 205–213, doi:10.1175/1520-0450(1997)036<0205:EOTWSF>2.0.CO;2.
- Lloyd, G., T. W. Choularton, K. N. Bower, M. W. Gallagher, P. J. Connolly, M. Flynn, R. Farrington, J. Crosier, O. Schlenczek, J. Fugal, and J. Henneberger (2015), The origins of ice crystals measured in mixed-phase clouds at the high-alpine site jungfraujoch, *Atmos. Chem. Phys.*, 15(22), 12,953–12,969, doi:10.5194/acp-15-12953-2015.
- Lohmann, U. (2002), Possible aerosol effects on ice clouds via contact nucleation, *Journal of the Atmospheric Sciences*, 59(3), 647–656, doi:10.1175/1520-0469(2001)059<0647:PAEOIC>2.0.CO;2.
- Lohmann, U., F. LÃijÃnd, and F. Mahrt (2016), *An Introduction to clouds: from the microscale to the climate*, Cambridge University Press, Cambridge, United Kingdom.
- Mahesh, A., R. Eager, J. R. Campbell, and J. D. Spinhirne (2003), Observations of blowing snow at the south pole, *Journal of Geophysical Research: Atmospheres*, 108(D22), n/a–n/a, doi:10.1029/2002JD003327, 4707.
- Nishimura, K., and M. Nemoto (2005), Blowing snow at mizuho station, antarctica, *Philosophical Transactions of the Royal Society of London A: Mathematical, Physical and Engineering Sciences*, 363(1832), 1647–1662, doi:10.1098/rsta.2005.1599.
- Palm, S. P., Y. Yang, J. D. Spinhirne, and A. Marshak (2011), Satellite remote sensing of blowing snow properties over antarctica, *Journal of Geophysical Research: Atmospheres*, 116(D16), n/a–n/a, doi:10.1029/2011JD015828, d16123.
- Rangno, A. L., and P. V. Hobbs (2001), Ice particles in stratiform clouds in the arctic and possible mechanisms for the production of high ice concentrations, *Journal of Geophysical Research: Atmospheres*, 106(D14), 15,065–15,075, doi:10.1029/2000JD900286.
- Rogers, D. C., and G. Vali (1987), Ice crystal production by mountain surfaces, *J. Clim. Appl. Meteorol.*, 26(9), 1152–1168, doi:10.1175/1520-

- 561 0450(1987)026<1152:ICPBMS>2.0.CO;2.
- 562 Rotunno, R., and R. A. Houze (2007), Lessons on orographic precipitation from the  
563 mesoscale alpine programme, *Quarterly Journal of the Royal Meteorological Society*,  
564 133(625), 811–830, doi:10.1002/qj.67.
- 565 Schlenzeck, O., and J. Fugal (2017), Microphysical properties of ice crystal precipitation  
566 and surface-generated ice crystals in a high alpine environment in switzerland, *esult*, 56,  
567 433–453, doi:10.1175/JAMC-D-16-0060.1.
- 568 Schmidt, R. A. (1982), Vertical profiles of wind speed, snow concentration, and  
569 humidity in blowing snow, *Boundary-Layer Meteorology*, 23(2), 223–246, doi:  
570 10.1007/BF00123299.
- 571 Vali, G., D. Leon, and J. R. Snider (2012), Ground-layer snow clouds, *Quarterly Journal*  
572 *of the Royal Meteorological Society*, 138(667), 1507–1525, doi:10.1002/qj.1882.
- 573 Vionnet, V., G. GuyomarcâŽh, F. N. Bouvet, E. Martin, Y. Durand, H. Bellot, C. Bel,  
574 and P. PugliaÃlise (2013), Occurrence of blowing snow events at an alpine site over a  
575 10-year period: Observations and modelling, *Advances in Water Resources*, 55, 53 – 63,  
576 doi:<http://doi.org/10.1016/j.advwatres.2012.05.004>, snowâŠAtmosphere Interactions  
577 and Hydrological Consequences.
- 578 Yang, J., and M. K. Yau (2008), A new triple-moment blowing snow model, *Boundary-*  
579 *Layer Meteorology*, 126(1), 137–155, doi:10.1007/s10546-007-9215-49.

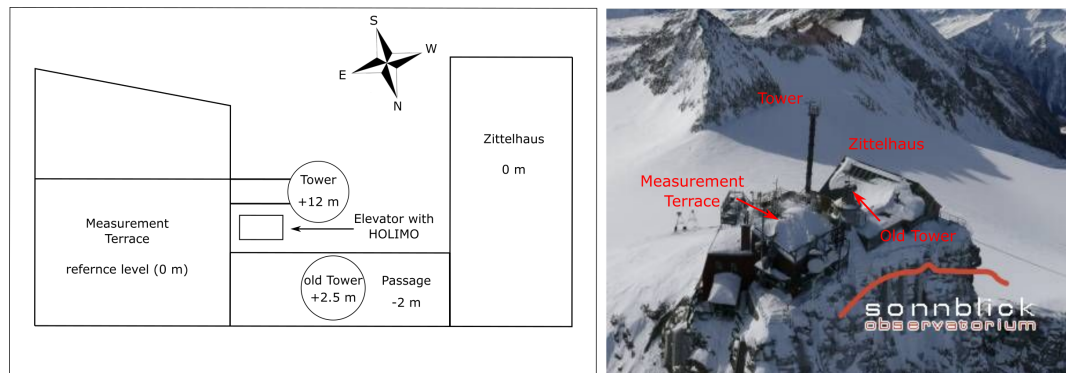


**Figure 1.** Sketch of the experimental setup and the surrounding structures (left) with their heights relative to the bottom of the measurement terrace. Aerial image of the Sonnblick Observatory (right).

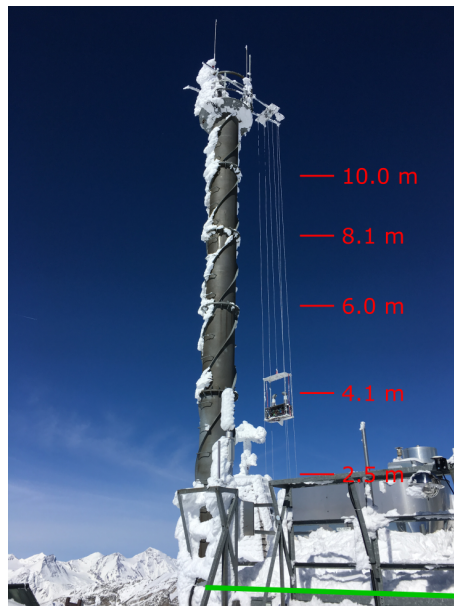
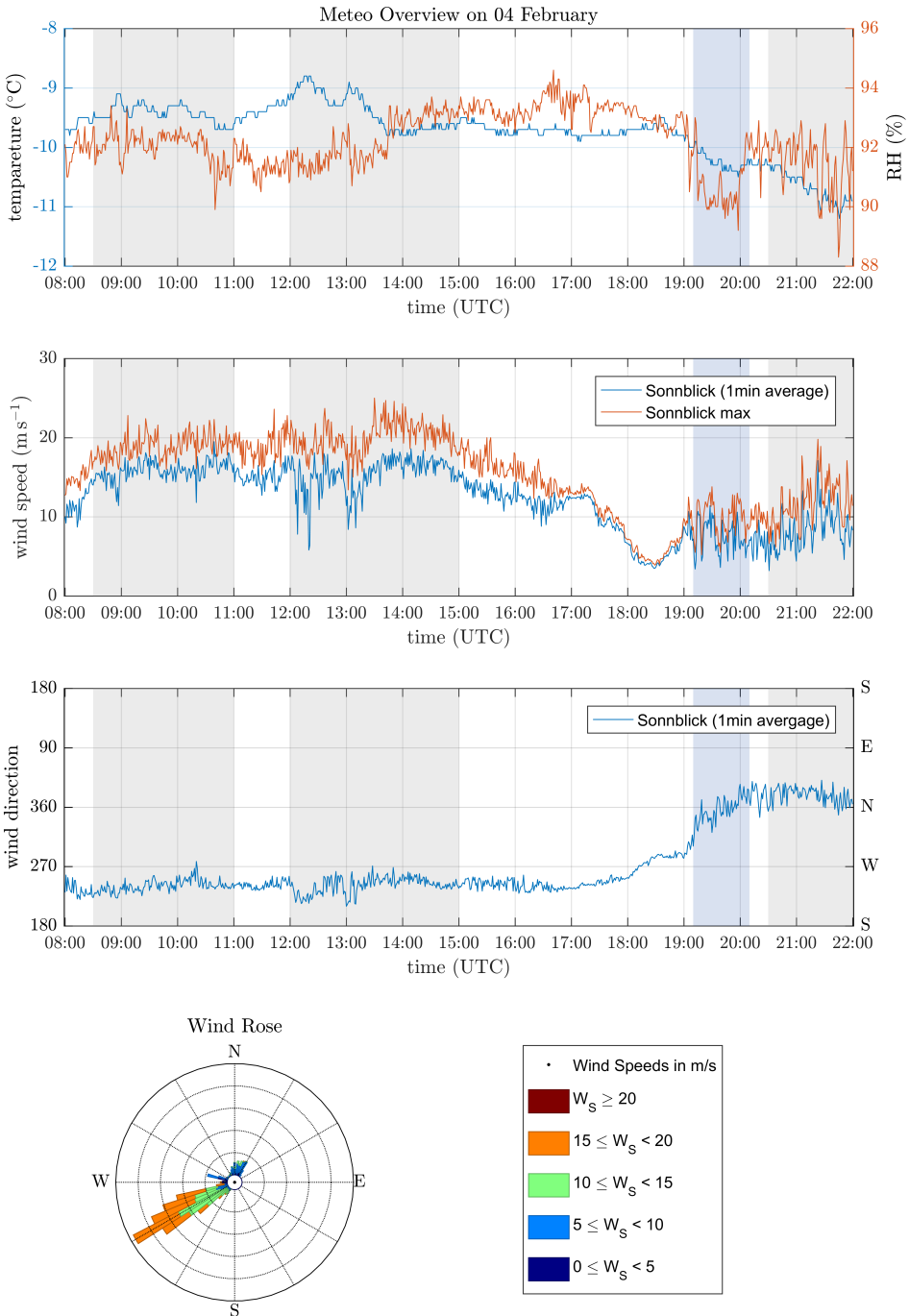
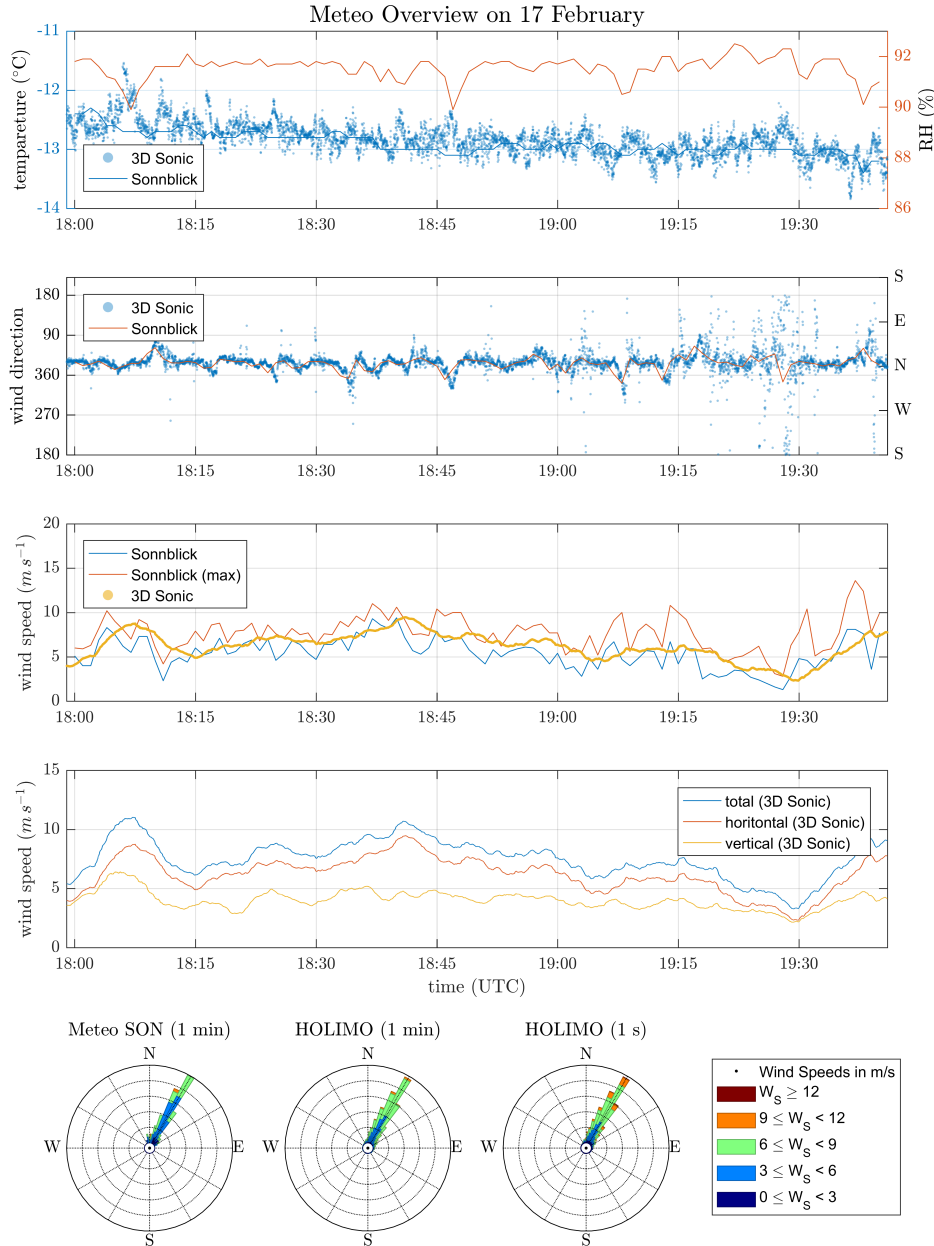


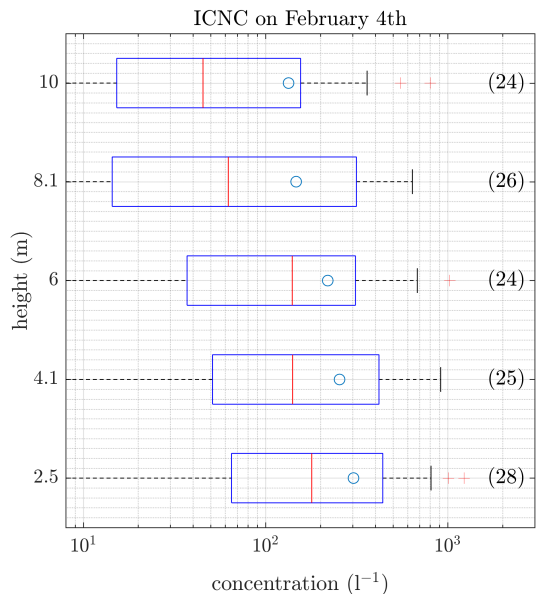
**Figure 2.** Set up of the elevator with the holographic imager HOLIMO mounted to the meteorological tower at the SBO. The red lines and numbers indicate the five different heights where the elevator was positioned repeatedly to obtain vertical profiles of the ICNC. The reference height of 0.0 m is the bottom of the measurement platform (green line).



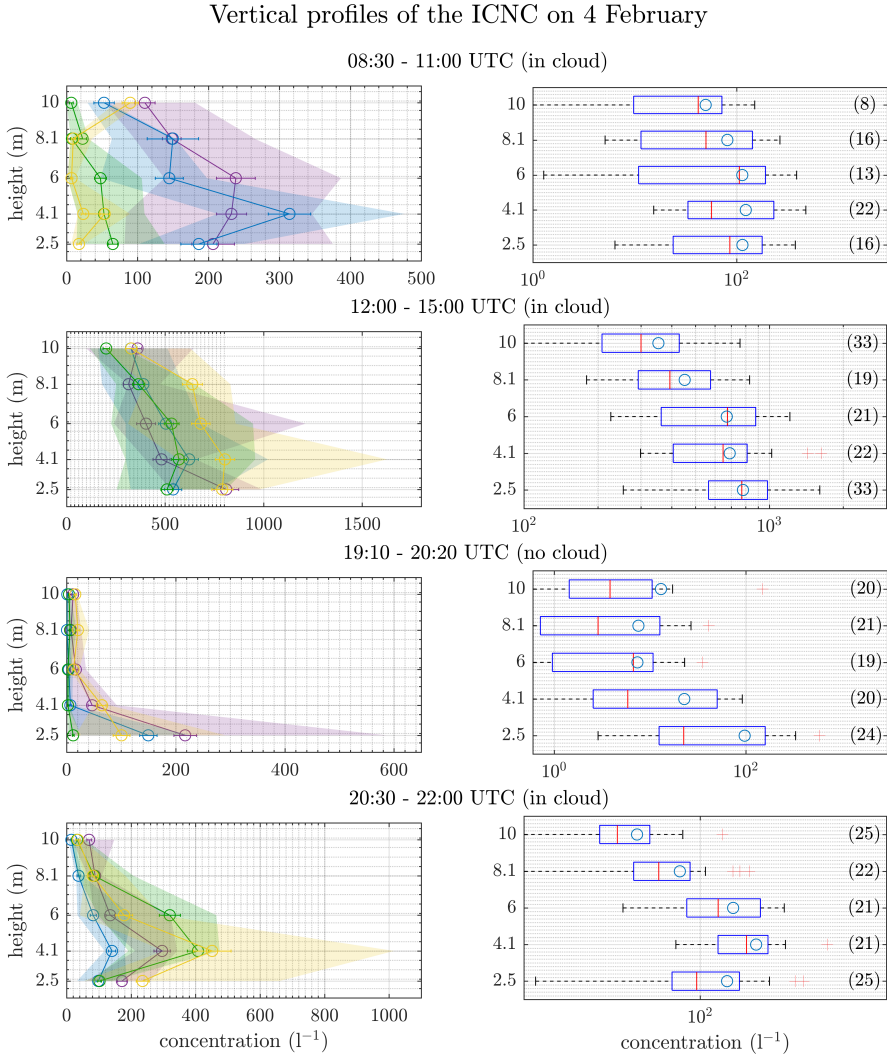
586 **Figure 3.** Overview of the meteorological conditions on 4 February, 2017 obtained from the SBO measure-  
 587 ments. All measurements are 1 min averages except for the maximum wind speed, which corresponds to the  
 588 maximum wind speed observed during a 1 min average. The shaded areas represent intervals with ice crystal  
 589 measurements with the SBO in cloud (gray), respectively not in cloud (blue). Shown are the temperature and  
 590 relative humidity (top), wind speed (second from top) and wind direction (second from bottom). A windrose  
 591 plot is shown in the bottom panel.



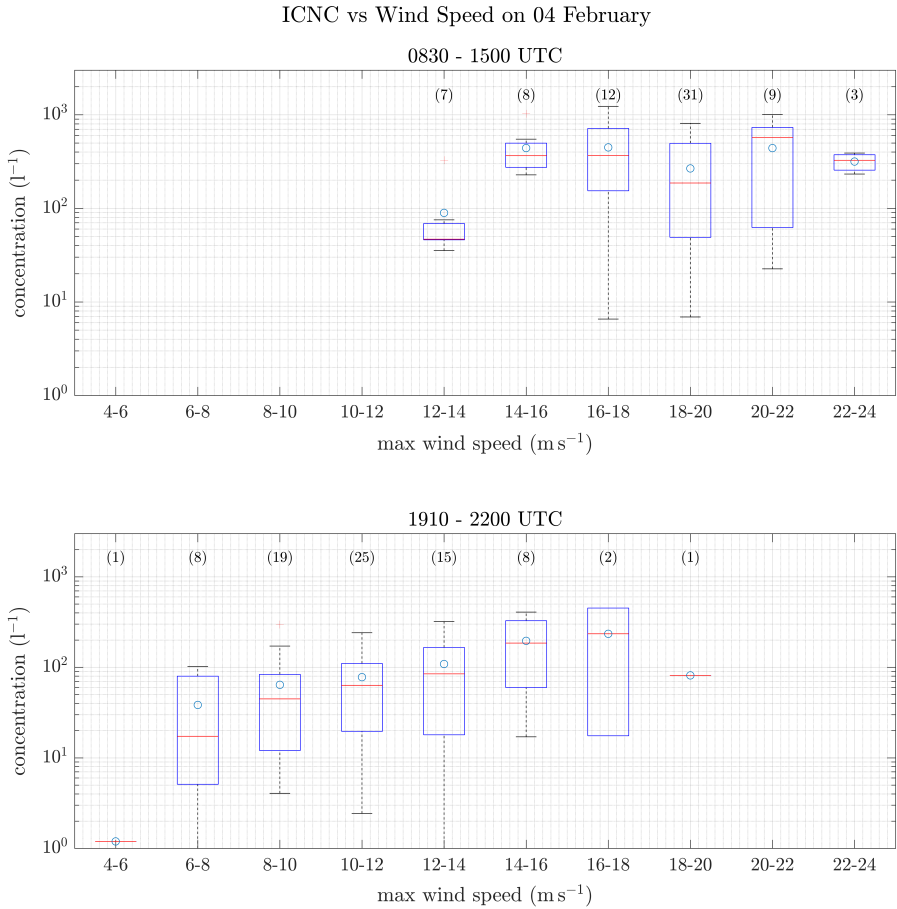
592 **Figure 4.** Overview on the meteorological conditions on 17 February, 2017 for the time interval when mea-  
 593 surements exist (see Fig. 8). On this day temperature and wind measurements are available from the SBO and  
 594 the 3D Sonic Anemometer. Shown are the temperature and relative humidity (top), wind direction (second  
 595 from top), a comparison of the horizontal wind speed (middle) and detailed wind speed measurements from  
 596 the 3D Sonic Anemometer (second from bottom). A windrose plot is shown in the bottom panel.



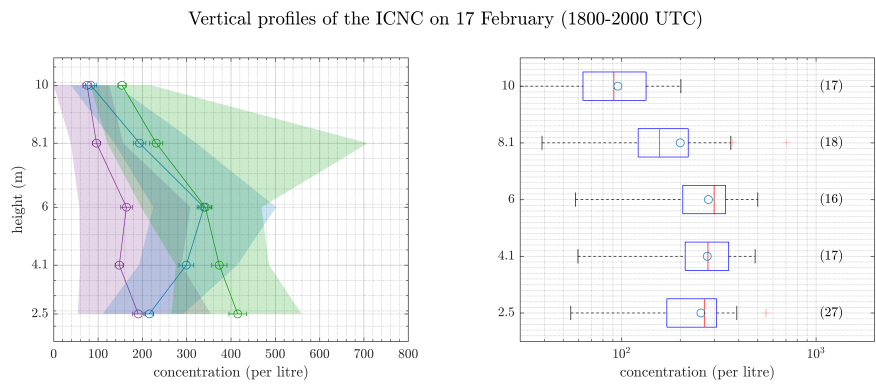
597 **Figure 5.** ICNC as a function of the height of the elevator at the meteorological tower of the SBO. This  
 598 plot is a summary of the 24 profiles obtained on 4 February, 2017. The data was averaged for each height over  
 599 the entire time period. The number in brackets is the number of concentration measurements per height. For  
 600 each box, the central line marks the median value of the measurement and the left and right edges of the box  
 601 represent 25th and the 75th percentiles, respectively. The whiskers extend to the minima and maxima of the  
 602 data; outliers are marked as red pluses. The mean values of the measurements are indicated as blue circles.



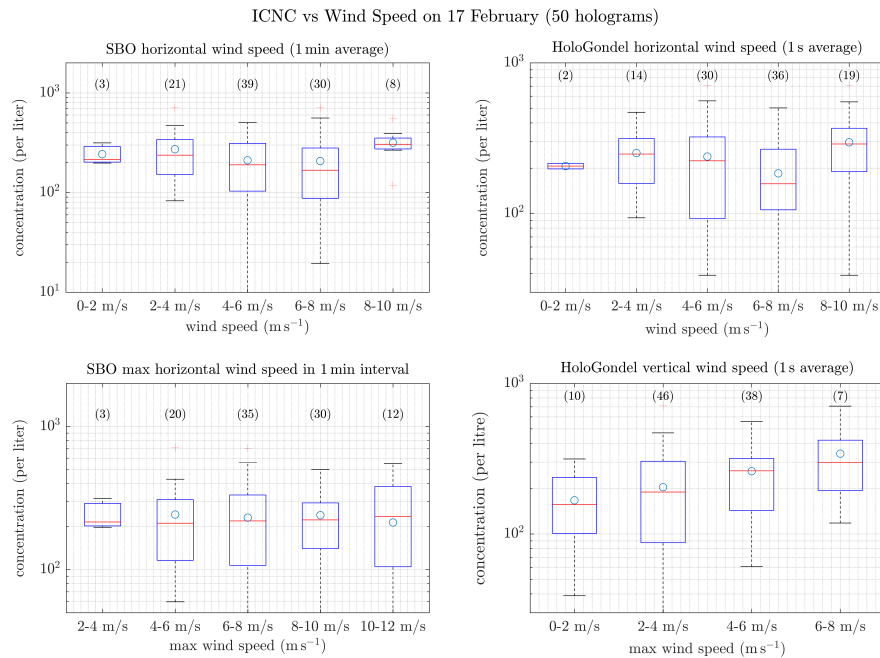
603 **Figure 6.** ICNCs as a function of height of the elevator for four different time intervals during 4 February,  
604 representing different conditions (Fig. 3). In the individual profiles (left), the circles indicate the mean and  
605 the error bars the standard error of the mean. The shaded areas extent from the minima to the maxima of the  
606 measured ICNC. The box plots (right) show a summary of all profiles in the respective time interval as in  
607 Figure 5.



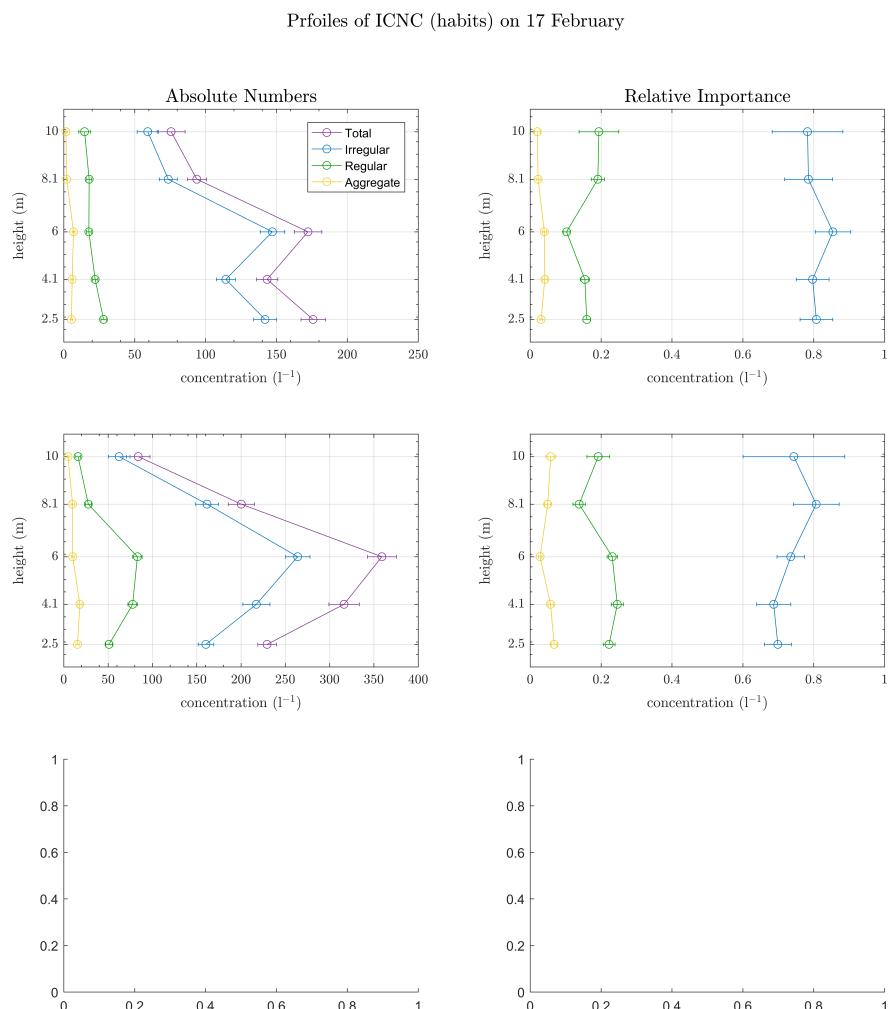
608 **Figure 7.** As Figure 5, but for ICNC as a function of the horizontal wind speed for the the time periods  
609 between 0830 and 1500 UTC when the wind direction was from the west-southwest (top) and between 1910  
610 and 2200 UTC when the wind direction was from the north (bottom). The ICNCs from HOLIMO are one  
611 minute averages and the wind speeds from the SBO are the maxima in the respective one minute intervals.



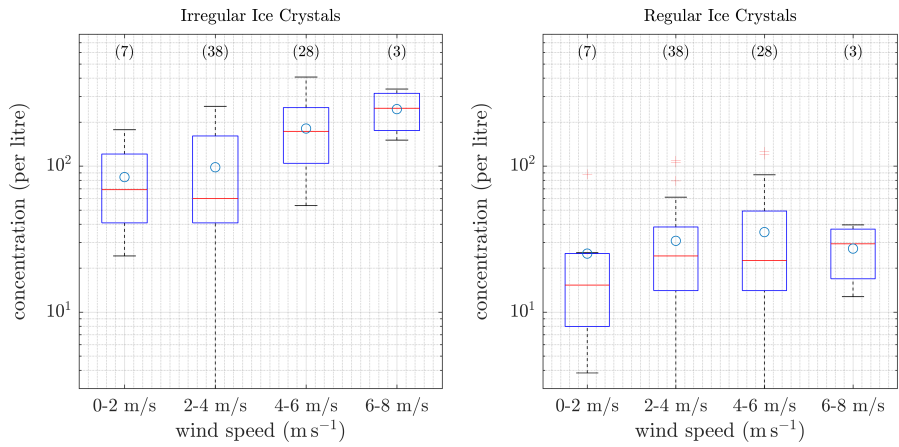
612 **Figure 8.** As Figure 6, but for ICNC as a function of height observed on 17 February, 2017.



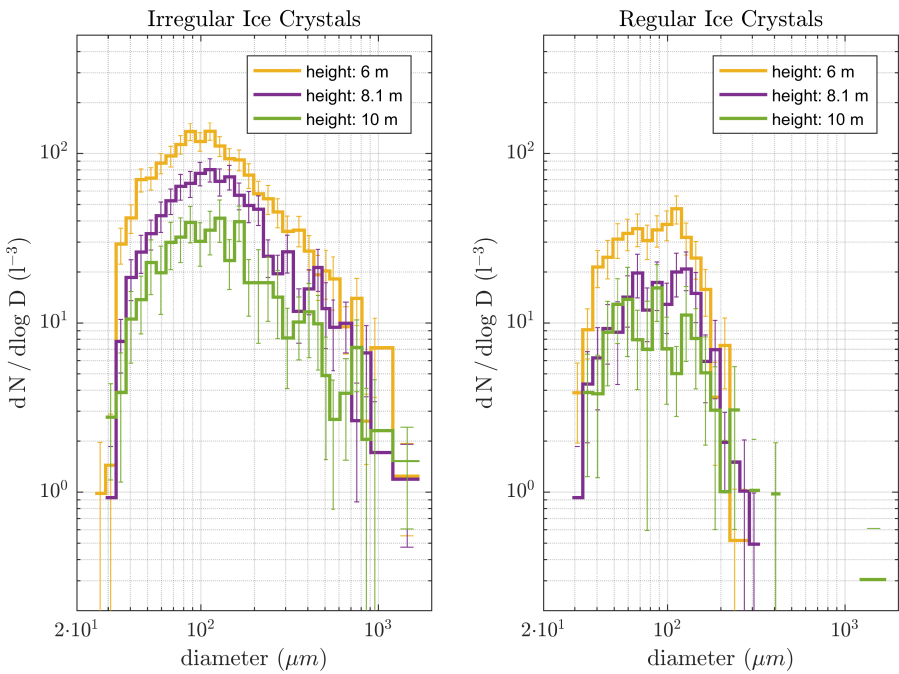
613 **Figure 9.** As Figure 7 only for 17 February and four different wind speed measurements: a) one minute  
 614 b) maximum wind speed of the a corresponding time  
 615 interval in a), c) secondly averages of the horizontal wind speed and d) secondly average of the vertical wind  
 616 speed both from the 3D Sonic Anemometer.



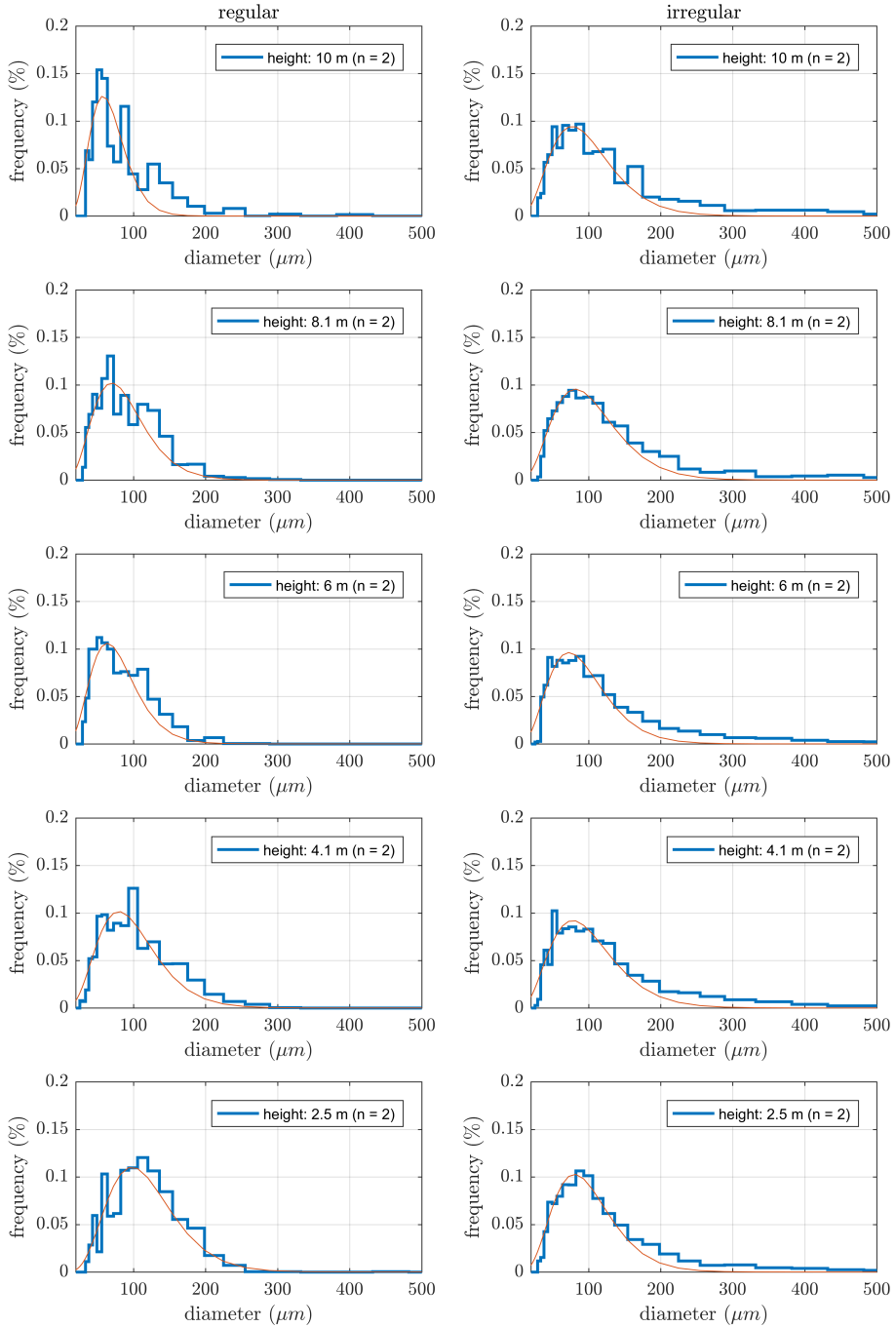
617 **Figure 10.** Vertical profiles of the concentration (left) and the fraction (right) of individual ice crystal  
 618 habits. For the fraction, the ICNC of individual habits were divided by the total ICNC. The circles represent  
 619 the mean and the error bars represent the standard error of the mean.



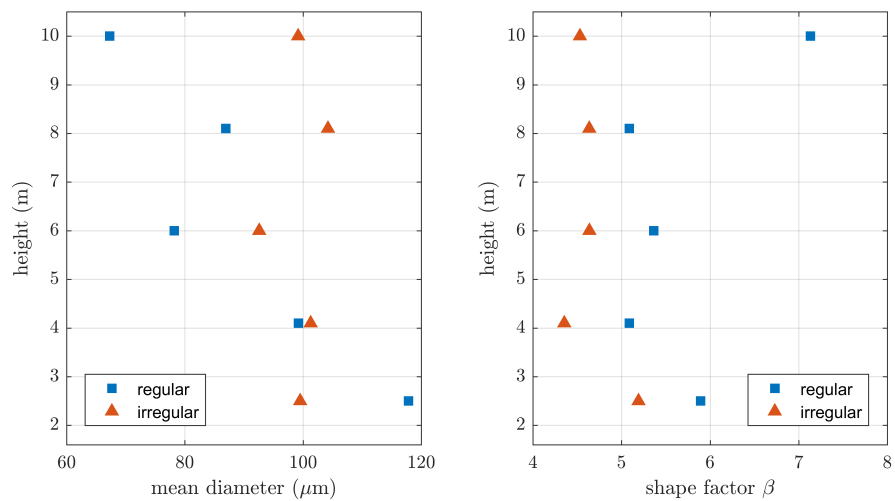
620 **Figure 11.** As Figure 7 only for 17 February, 2017, for the ICNC of different ice crystal habits as a function  
621 of the vertical wind speed. Aggregates are not shown because of their very low concentrations.



622 **Figure 12.** Size distribution of the irregular (left) and regular (right) ice crystals observed on 17 February,  
623 2017 as a function of height. The error bars represent the standard error of the mean. Aggregates are not  
624 shown because of their very low concentrations.



625 **Figure 13.** Probability distribution of the particle diameter for regular (left)  
626 and irregular (right) ice crystals  
627 measured on 17 February, 2017. The red lines indicate the result of the fit of the two parameter gamma probability density function from equation (1). Aggregates are not shown because of their very low concentrations.



628 **Figure 14.** Profiles of the mean diameter (left) and the shape parameter (right)  
629 probability density function (Eq. (1)) plotted as a function of height.